Appl. Phys. B 84, 295–302 (2006)
DOI: 10.1007/s00340-006-2256-4

Applied Physics B
Lasers and Optics

R.A. GANEEV[1,2,✉]
A.I. RYASNYANSKY[3]

Nonlinear optical characteristics of nanoparticles in suspensions and solid matrices

[1] Akadempribor Scientific Association, Academy of Sciences of Uzbekistan, Akademgorodok, Tashkent 700125, Uzbekistan
[2] The Institute for Solid State Physics, The University of Tokyo, 5-1-5 Kashiwanoha, Kashiwa, Chiba 277-8581, Japan
[3] Samarkand State University, Samarkand 703004, Uzbekistan

Received: 30 November 2005/Revised: 11 April 2006
Published online: 5 May 2006 • © Springer-Verlag 2006

ABSTRACT The study of the nonlinear optical parameters of suspensions and glass matrices doped with various nanoparticles (Ag, Cu, Co, Au, Pt, GaAs, CdS, As_2S_3) are presented. Various techniques for the preparation of nanoparticles in suspensions and solid matrices, in particular laser ablation, chemical methods, and ion implantation are discussed. We present our measurements of the nonlinear refractive indices, nonlinear absorption coefficients, saturation intensities, and nonlinear susceptibilities of nanoparticles-containing media using laser pulses generating in various spectral and temporal ranges.

PACS 42.65.An; 42.65.Hw; 42.65.Jx; 61.46.Df; 78.67.Bf

1 Introduction

The nonlinearities of nanostructured materials has attracted interest due to the considerable enhancement of their nonlinear response caused by quantum size effects [1]. The application of such structures to optoelectronics, optical switchers and limiters, etc. [2–4], as well as in optical computers, optical memory, and nonlinear spectroscopy can considerably enhance their effectiveness.

In this paper, we present the nonlinear optical studies of semiconductor- and metal-based nanoparticles (Ag, Cu, Au, Pt, Co, GaAs, As_2S_3, CdS) in various materials. Some of these media could be considered as the possible optical limiters of intense laser radiation. We present our measurements of their nonlinear refractive indices γ, nonlinear absorption coefficients β, saturation intensities I_s, and nonlinear susceptibilities $\chi^{(3)}$ using different spectral and temporal ranges of the probe radiation.

2 Basic relations

In general case, the medium's refractive index n can be written as follows

$$n = n_0 + \gamma I + \eta I^2 + \dots , \tag{1}$$

where n_0 is the linear term of the refractive index of medium, I is the intensity of the electromagnetic wave, and η is the fifth-order nonlinear refractive index.

✉ Fax: +998711690124, E-mail: rashid_ganeev@yahoo.com

In the case of the linear dependence of the absorption coefficient on the laser radiation intensity one can use the following equation:

$$\alpha(I) = \alpha_0 + \beta I , \tag{2}$$

where α_0 is the linear term of the absorption coefficient of the medium.

The calculations of the real and imaginary parts of nonlinear susceptibility were carried out using the relations

$$\mathrm{Re}\chi^{(3)} = 10^{-6} c n_0^2 \gamma / 480\pi^2 \tag{3}$$

and

$$\mathrm{Im}\chi^{(3)} = 10^{-7} c^2 n_0^2 \beta / 96\pi^2 \omega , \tag{4}$$

where c is the light velocity in cm s^{-1}, ω is the laser radiation frequency in cycles s^{-1}, β is the nonlinear absorption coefficient in cm W^{-1}, and γ is the nonlinear refractive index in cm^2 W^{-1}.

One of the advantages of the z-scan technique commonly used for the measurements of the nonlinear optical properties of media is a possibility of defining the contribution of several nonlinearities when they are simultaneously present. In general, when both nonlinear refraction and absorption are present, the normalized transmittance T of nonlinear medium can be written as follows [5]:

$$T = 1 - \frac{4x}{(x^2+9)(x^2+1)}\Delta\Phi_0 - \frac{2(x^2+3)}{(x^2+9)(x^2+1)}\Delta\Psi_0 , \tag{5}$$

where $x = z/z_0$, $z_0 = 0.5kw_0^2$ is the diffraction length, $k = 2\pi/\lambda$ is the wavenumber, w_0 is the beam waist radius, $\Delta\Phi_0$ and $\Delta\Psi_0$ are the parameters which determine the phase shift near the focus as a result of nonlinear refraction and absorption, $\Delta\Phi_0 = k\gamma I_0 L_{\mathrm{eff}}$, $\Delta\psi_0 = \beta I_0 L_{\mathrm{eff}}/2$, I_0 is the laser radiation intensity in the focus, $L_{\mathrm{eff}} = [1 - \exp(-\alpha_0 L)]/\alpha_0$ is the effective length of the sample, and L is the sample length. Writing the following expression: $\varrho = \beta/2k\gamma$, one can get the relation between $\Delta\Phi_0$ and $\Delta\Psi_0 (\Delta\Psi_0 = \varrho\Delta\Phi_0)$. In this case (5) can be rewritten in the following form:

$$T = 1 - \frac{2(\varrho x^2 + 2x + 3\varrho)}{(x^2+9)(x^2+1)}\Delta\Phi_0 \tag{6}$$

The best fitting of theory and experiment can be observed at the specific values of ϱ and $\Delta\Phi_0$. Using ϱ and $\Delta\Phi_0$ as the parameters, the $\Delta\Psi_0$ value was determined. Further, by subtracting the nonlinear absorption from (5), one can calculate the nonlinear refraction of samples.

3 Experimental arrangements

In our work we used three lasers operating at different lasing conditions. A picosecond Nd:YAG laser at a 2 Hz pulse repetition rate was used in most of our experiments. A single pulse ($t = 55$ ps, or in some cases 35 ps) was amplified up to the energy of $E = 2$ mJ. The nonlinear optical characteristics of nanoparticle-containing samples were investigated at the wavelength of this laser ($\lambda = 1064$ nm) and its second harmonic ($\lambda = 532$ nm, $E = 0.2$ mJ). We also used a Ti:sapphire laser delivering femtosecond pulses ($t = 110$ fs, $\lambda = 795$ nm, $E = 10$ mJ) at a 10 Hz pulse repetition rate. The variation of the distance between the gratings of the compressor of this laser allowed generation of pulses with variable duration (from 110 fs to 1.6 ps). This laser also operated at a Q-switching regime producing 8 ns pulses. Pulses of 80 MHz, 100 fs, 300 mW frequencies were also available from the seeding oscillator (Tsunami) of this laser for the investigation of thermally induced self-defocusing of various nanoparticle-containing media. The third laser was a hybrid Nd:glass–Ti:sapphire laser generating 475 fs, 1054 nm, 0.1 mJ pulses at a 1 Hz repetition rate.

The laser radiation was focused by a 30 cm focal length lens FL (Fig. 1). The nanoparticle-containing objects under study S were moved using a translation system TS along the optical Z-axis through the focusing area. The maximum radiation intensity was varied in the range of 4×10^8–4×10^{10} W cm^{-2}. Its value depended on the optical breakdown and multiphoton ionization thresholds of the media. The energy of the laser pulses were measured using a calibrated photodiode PD1 and recorded by a digital voltmeter DV1. Calibrated neutral filters varied the laser radiation energy. A 1 mm aperture A transmitting 2% of the laser radiation was set at a distance of 100 cm from the focusing area (the closed-aperture scheme). A photodiode PD2 was placed behind the aperture and the propagated radiation was recorded by a digital voltmeter DV2. In order to exclude the influence of the instability of laser radiation on the measurement of the nonlinear optical parameters of samples, a signal detected by the PD2 was normalized by a signal detected by the PD1.

The closed-aperture scheme was capable of determining both the sign and magnitude of the γ of materials using the normalized transmittance dependencies $T(z)$. The nonlinear absorption coefficient was measured using the open-aperture scheme, when the sample's transmission was measured without the aperture. In this case, a detector measuring the energy of the propagated beam had a sufficiently broad aperture and was placed at such a distance from the sample that the transmitted radiation was entirely detected. A controller C collected the measured signals from the voltmeters. The controller was used for the analysis of the information from the voltmeter outputs and the operation of a translation system. The translation system consisted of a micrometer and step motor and provided a step movement of 20 μm/cycle. The data processing procedure included the averaging of measurements over the software-specified number of laser shots at a given coordinate Z and the exclusion of certain measurements at significant intensity fluctuations of the incident radiation. Twenty separate measurements were performed at a fixed position of the sample. This allowed a total error decrease in transmission measurements to 2%. A personal computer (PC) carried out the general control over experimental set-up. The calibration of nonlinear optical parameters was carried out using a CS_2 [6].

4 Metal nanoparticles (Ag, Cu, Co, Au, Pt)

4.1 *Ablated silver suspensions*

Silver nanoparticles have an advantage over other metal nanoparticles (i.e., gold and copper) since the surface plasmon resonance (SPR) of Ag is located far from the interband transitions. This means that, in the case of silver nanoparticle-containing compounds, we can investigate the nonlinear optical effects solely using the surface plasmon contribution. Here we present our studies of the optical, structural, and nonlinear optical properties of the Ag nanoparticles prepared by laser ablation in various liquids. The laser ablation of silver was performed using a second-harmonic

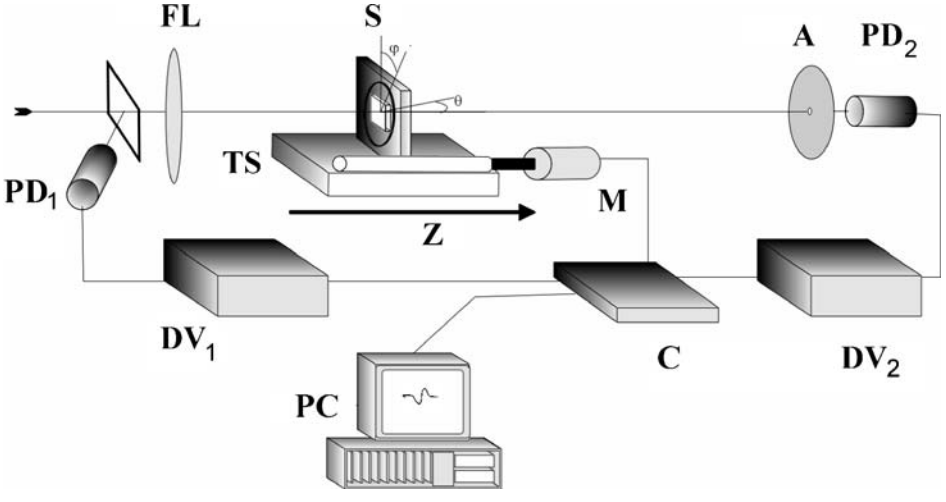

FIGURE 1 Experimental setup. FL: focusing lens; BS: beam splitter; S: investigated sample; PD1, PD2: photodiodes; DV1, DV2: digital voltmeters; M: step motor; TS: translation system; C: controller; PC: personal computer; A: aperture

radiation of Q-switched Nd:YAG laser. The laser radiation ($\lambda = 532$ nm, $t = 9$ ns, $E = 30$ mJ, 10 Hz pulse repetition rate) was focused by a 50 mm focal length lens on the surface of a silver block placed inside a 10 mm thick cell. The cells were filled with the liquids possessing different viscosities (ethylene glycol, water, and ethanol). The energy density of the 532 nm radiation at the target surface was measured to be $20\,\mathrm{J\,cm^{-2}}$. The ablated silver suspensions were then studied using the laser pulses generated in different spectral and temporal ranges to measure the nonlinear optical characteristics.

The appearance of stable Ag nanoparticles was confirmed by TEM studies of these suspensions. The TEM measurements conducted just after laser ablation showed the appearance of nanoparticles with a size distribution ranging from 4 to 200 nm. After half a month this distribution was considerably narrowed with just small nanoparticles (ranging from 5 to 10 nm) dominating in the ablated suspension. In the inset in Fig. 2, curve 1 shows the absorption spectrum of the silver ablated in ethylene glycol. The absorption curve was centered in the vicinity of the SPR of Ag (405 nm), which indicated the appearance of small nanoparticles. The variations of the absorption spectra of the ablated nanoparticles were observed during a period of one month (see curves 1–3). The initial absorption spectra of the silver ablated in different liquids (water, ethylene glycol, ethanol) were similar. However, the absorption of Ag:water and Ag:ethanol suspensions was weakened after two weeks as compared to the Ag:ethylene glycol (Ag:EG) suspension, probably due to the higher viscosity of ethylene glycol, which prevented the nanoparticles from sedmenting.

The previously reported influence of thermal accumulative effects on the behavior of nonlinear optical refraction in various media at high repetition rates of femtosecond pulses (of the order of tens of MHz) has shown the importance of heat accumulation between the pulses due to various (linear and/or nonlinear) mechanisms of optical losses. We used the radiation of a Ti:sapphire oscillator ($\lambda = 795$ nm, $W = 300$ mW, $t = 100$ fs, 80 MHz pulse repetition rate) to analyze the influence of thermally induced nonlinearities on the propagation of laser radiation through Ag-containing suspensions. The analysis of CCD images using the z-scan scheme showed a presence of the thermal lens. The thermally induced nonlinear refractive index of Ag:EG suspension in the case of a high pulse repetition rate was measured to be $\gamma = -8 \times 10^{-12}\,\mathrm{cm^2\,W^{-1}}$.

In the next set of nonlinear optical studies we used radiation operating at 1 and 10 Hz pulse repetition rates to exclude the influence of thermal accumulative processes. In the case of the second-harmonic radiation of a nanosecond Nd:YAG laser ($\lambda = 532$ nm, $t = 8$ ns, $E = 2$ mJ, 1 Hz pulse repetition rate) we did not observe the fast Kerr-induced nonlinear optical processes in Ag-containing suspensions up to the maximum intensities of $I_0 = 8 \times 10^9\,\mathrm{W\,cm^{-2}}$. These studies were carried out using the closed-aperture z-scan scheme and time-integrated photodiodes. However, self-defocusing was observed when we analyzed the waveform of the propagated pulses using fast pin diodes by applying a technique developed in [7, 8]. Our studies have shown that this process was caused by physical mechanisms other than those that were observed in the case of the high pulse repetition rate. In the latter case the appearance of a negative lens was caused by a heat accumulation, whereas in the former case the self-defocusing was attributed to the acoustic wave propagation through the beam waist area [8].

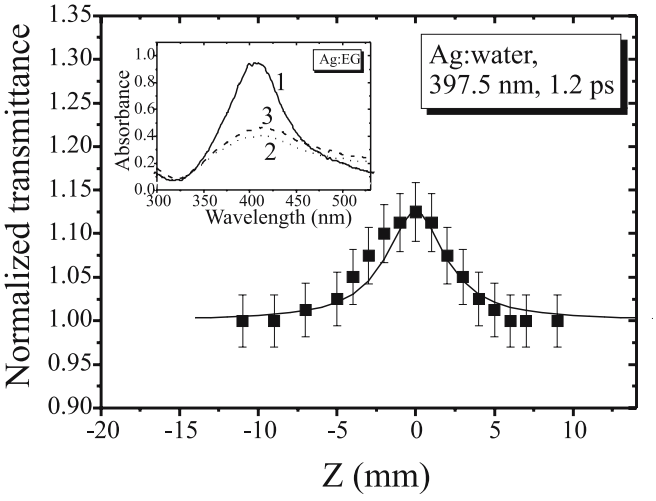

FIGURE 2 Normalized transmittance of Ag:water suspension in the case of open-aperture scheme. *Inset*: Absorption spectra of Ag:EG suspension (1: initial spectrum after ablation; 2: after one week; 3: after three weeks)

The open-aperture z-scans of Ag-containing suspensions were carried out using 397.5 nm, 8 ns radiation. We assumed that, in the case of long pulses, the reverse saturated absorption plays an important role in the overall dynamics of the nonlinear optical transmittance of nanoparticle-containing compounds in the UV range, taking into account a saturation of the intermediate states responsible for the saturated absorption in the case of femtosecond and picosecond pulses. The nonlinear absorption coefficient of an Ag:water suspension at $\lambda = 397.5$ nm was measured to be $3 \times 10^{-9}\,\mathrm{cm\,W^{-1}}$.

The only nonlinear optical process observed at $\lambda = 795$ nm in the silver suspensions was a nonlinear absorption caused by two-photon processes in these compounds. The nonlinear absorption coefficient of the Ag:water suspension was measured to be $8 \times 10^{-9}\,\mathrm{cm\,W^{-1}}$ (at $\lambda = 795$ nm, $t = 800$ fs). In the case of 397.5 nm, 1.2 ps radiation, a weak positive nonlinear refraction was registered in the closed-aperture z-scans. The γ and $\mathrm{Re}\chi^{(3)}$ of the Ag:water suspension were calculated to be $3 \times 10^{-13}\,\mathrm{cm^2\,W^{-1}}$ and 2×10^{-12} esu, respectively.

The saturated absorption of the Ag nanoparticles embedded in silica glass matrices was previously observed as far as 355 nm. We also registered this process in Ag:water suspension in the case of 397.5 nm, 1.2 ps radiation (Fig. 2). The solid line in Fig. 2 was calculated by setting $\beta = -1.5 \times 10^{-9}\,\mathrm{cm\,W^{-1}}$. The I_s was evaluated to be $6 \times 10^8\,\mathrm{W\,cm^{-2}}$. We estimated the third-order susceptibility of the nanoparticles to be $\left|\chi^{(3)}\right| \sim 5 \times 10^{-8}$ esu, assuming a small volume ratio of silver in the liquid suspensions (4×10^{-5}).

4.2 *Colloidal metals prepared by chemical methods*

Colloidal metals demonstrate high nonlinearity and a fast response, especially in the vicinity of SPRs. The dynamics of the spatial parameters of aggregated particles leads

to the variations of their nonlinear optical characteristics. At the same time, the physical nature of the variation of colloidal metals' nonlinear refractive indices remains unclear.

We present below, the results of the study of the nonlinear optical parameters of the colloidal metal suspensions (silver, gold, and copper), prepared by chemical methods at the wavelengths of the Nd:YAG laser and its second-harmonic generated in different timescales ($\lambda = 1064$ nm and 532 nm, $t = 35$ ps and 28 ns). To prepare the colloidal gold, 30 ml of 1% sodium citrate solution was added to 250 ml of boiling tetrachloroauric acid solution. The mixture was boiled until a deep wine red color was obtained, indicating the formation of the colloidal gold suspension. For the preparation of the colloidal Cu suspension we dissolved 4 g of $CuSO_4$ in a liter of distilled water. For the preparation of the Ag suspension we dissolved 20 mg of collargol in 200 ml of distilled water and heated this solution at 90 °C. Electron microscopy analysis of silver fractal containing suspensions at the different stages of aggregation showed the presence of the nanoparticle with sizes that varied from 10 nm (for the non-aggregated state) to 40–100 nm (for the aggregated state). Other samples also showed the presence of nanosized structures.

All the colloidal suspensions excluding the gold one, showed a positive nonlinear refraction at $\lambda = 1064$ nm. The same picture was observed at $\lambda = 532$ nm except for the copper suspension, where the nonlinear refraction changed its sign from positive (at 1064 nm) to negative (at 532 nm). The nonlinear absorption of picosecond pulses was observed in the case of colloidal gold. The nonlinear absorption coefficients for colloidal gold were measured to be 1×10^{-12} cm W^{-1} (at $\lambda = 1064$ nm, $t = 35$ ps) and 9.4×10^{-12} cm W^{-1} (at $\lambda = 532$ nm, $t = 35$ ps).

Our studies of colloidal metals using the nanosecond pulses showed that their nonlinear susceptibilities were two to three orders of magnitude higher than those measured using the picosecond pulses. In the case of nanosecond pulses, we observed a variation of the pulse shape after the propagation of radiation through the cell and aperture, indicating the influence of a thermal effect. The dynamics of the nonlinear optical parameters with the growth of aggregation remained the same as for the picosecond pulses. It should be noted that, in the case of nanosecond pulses, we did not observe a nonlinear absorption up to the maximum intensities used ($I = 8 \times 10^9$ W cm^{-2}), which was considerably smaller than the maximum intensity of the picosecond pulses ($I_0 = 4 \times 10^{11}$ W cm^{-2}). The γ of silver colloids in this case was measured to be -9×10^{-13} cm^2 W^{-1}.

The colloidal solution of metallic platinum was prepared in the following way. The initial material for the preparation of a reference colloidal solution was metallic platinum, 0.1 g of which upon heating was dissolved in several milliliters of a mixture of nitric and hydrochloric acids. After evaporation of the solution, the dry residue was again dissolved in 20 ml of diluted (1 : 1) hydrochloric acid. After dissolution in the distilled water, one milliliter of the aqueous solution of this compound contained one milligram of platinum. According to the TEM analysis, the dimensions of Pt clusters ranged from 10 to 60 nm, depending on the degree of metal aggregation.

The nonlinear optical susceptibility of this compound was determined from the third harmonic generation (THG) measurements. The dependence of the third harmonic (TH) intensity on the fundamental radiation intensity $I_{3\omega}(I)$ was measured using the Nd:YAG laser ($\lambda = 1064$ nm, $t = 35$ ps). The slope of this dependence remained close to 2.8 up to $I = 5 \times 10^{10}$ W cm^{-2}.

The phase-matching conditions ($\Delta k = k_3 - 3k_1 = 0$, where k_1 and k_3 are the wave vectors of fundamental and harmonic radiation), which are also determined by the fundamental radiation focusing parameters should be fulfilled for efficient frequency conversion. In our experiments, the laser radiation was focused by a 25 cm focal length lens. A confocal parameter of focusing radiation was measured to be $b = 6$ mm. The thickness of the nonlinear medium was 1 mm, i.e. the conversion process took place under the conditions of weak focusing. In this case the phase matching conditions for the THG take place in the region of negative dispersion of investigated medium [9]. The Pt-containing colloids possess a positive dispersion for the THG in the region of the TH ($\lambda = 354.7$ nm). This conclusion was drawn on the basis of the absorption spectra investigations. The phase-matching condition was not fulfilled for the observed process. The value of the TH intensity in this case is defined as follows [10]:

$$I_{3\omega} = \gamma^2 l^2 I_{10}^3 \exp(-6k_1 r^2/b) \frac{\sin^2 \Delta(l, r)}{\Delta^2(l, r)}. \tag{7}$$

Here $\gamma_1 = 24\pi^3 \chi^{(3)}(-3\omega; \omega, \omega, \omega)/(n_1^{3/2} n_3^{1/2} c\lambda_1)$; $\Delta(l, r) = 2b/l - \alpha_1 - \beta$; $\alpha_1 = 2l\Delta k$ is the normalized phase-mismatching; $\beta = 72\pi^3 l \Delta\chi_k I_{10} \exp(-2k_1 r^2/b)/(n_1^2 c\lambda_1)$; $\Delta\chi_k = \chi^{(3)}(-\omega; \omega, \omega, -\omega)/2 - n_1 \chi^{(3)}(-3\omega; 3\omega, \omega, -\omega)/n_3$ is the difference of the Kerr-induced nonlinearities responsible for refraction index changes at the wavelengths of fundamental and harmonic radiation in the fundamental field; λ_i, k_i and n_i are the wavelengths, the wave numbers, and the refraction indices at a frequency of i-radiation, I_{10} is the maximal intensity at the plane of the beam waist, and l is the thickness of nonlinear medium.

This equation is fulfilled under low influence of the self-interaction effects ($|\beta| \ll b/l$). For the calculation of the THG at the strong influence of the self-interaction processes, we used more complicated equations, which took in to account the variations of the wave fronts of the interacted pulses (effects of self-focusing and self-defocusing). Equation (7) was integrated for the calculation of the THG conversion efficiency.

Parameter α_1 in our experiments did not exceed 0.05, thus the phase mismatching and linear absorption of the Co-containing solution should not drastically influence the frequency conversion. Under these conditions, the dependence of the TH intensity on the nonlinear medium concentration should be close to quadratic which agreed with our experiments. The dependence of the TH intensity on fundamental radiation at small intensities of pump radiation should have a cubic slope, which was also confirmed by the experimental data.

The growth of laser intensity ($I > 5 \times 10^{10}$ W cm^{-2}) led to a declination from the cubic slope. In our experiments the radiation intensity was below the optical damage threshold of the Pt-containing suspension ($I_{od} = 7 \times 10^{11}$ W cm^{-2}). Probably, the reason for the observed declination from the cubic

dependence is due to the influence of Kerr-induced nonlinearity that leads to the variations of the phase relation between the fundamental and generated radiation. With the increase of intensity the refractive indices change at the wavelengths of fundamental and TH radiation. The investigated slope of $I_{3\omega}(I)$ dependence can be both increased and decreased depending on the sign of the nonlinear refractive index.

The analysis of (7) also shows that, with the growth of fundamental intensity, the slope of the $I_{3\omega}(I_\omega)$ dependence slightly declines from the cubic one due to the Kerr-induced nonlinearities responsible for the changes of refractive indices at the fundamental and TH wavelengths. The maximum THG conversion efficiency for colloidal platinum was measured to be 7×10^{-7}. No TH signal was detected for other investigated metal-containing colloids (colloidal gold and colloidal silver). Taking into account our experimental conditions and (1), the nonlinear susceptibility of colloidal platinum $\chi^{(3)}(-3\omega; \omega, \omega, \omega)$ was measured to be 1.5×10^{-14} esu.

4.3 *Metal-doped glasses*

Metal-doped insulator matrixes attracted attention more than two decades ago [11]. These investigations are of great interest nowadays [4, 12–14] due to the potential applications of such materials as ultrafast optical switching systems and optical limiters. Here we present the results of our studies of the nonlinear optical properties of the copper and silver nanoparticles implanted in glass matrixes. The silica glasses (SG) containing 100% SiO_2 and the soda-lime silicate glasses (SLSG) containing 70% SiO_2, 20% Na_2O, and 10% CaO were used as the matrices for the preparation of the composite materials. These glasses were prepared as 1 mm (SG) and 3 mm (SLSG) thick plates. 60 keV ions at doses of 4×10^{16} and 8×10^{16} ions/cm^2 were used for the implantation of Ag^+ and Cu^+, respectively. The depth of implantation of the metal nanoparticles was measured to be 60 nm. X-ray reflectometry showed the average sizes of the Cu nanoparticles to be in the range of 3–5 nm. The silver-implanted samples were characterized by a broader size distribution of nanoparticles (from 2 to 18 nm) [15, 16]. The formation of metal nanoparticles was also proven by the appearance of selective absorption lines in optical transmission spectra with absorption maxima in the ranges of 400–450 nm (for silver-doped glasses) and 550–600 nm (for copper-doped glasses) corresponding to the SPRs of silver and copper nanoparticles.

We used the radiation of the Nd:YAG laser as well as its second- and third-harmonic radiation for the analysis of the nonlinearities of these samples in different spectral ranges. The output characteristics of the Nd:YAG laser radiation ($\lambda = 1064$ nm) were as follows: $t = 55$ ps, $E = 1$ mJ, at a 2 Hz pulse repetition rate. A peculiarity of copper-doped glasses was a difference in the sign of the γ of SG and SLSG glasses at the same implantation conditions. Cu:SG and Cu:SLSG samples were characterized by the self-defocusing and self-focusing properties, respectively, thus showing the importance of the matrix in the determination of the nonlinear optical process. We defined the γ of SLSG and Cu:SLSG to be 2.3×10^{-16} and 1×10^{-10} cm^2 W^{-1}, respectively. The values of β for Cu:SLSG and Cu:SG were measured to be 3.4×10^{-6} and 9×10^{-6} cm W^{-1}, respectively. The corresponding absolute value of the nonlinear susceptibility of Cu:SG was calculated to be $|\chi^{(3)}| = 2.4 \times 10^{-8}$ esu.

The self-focusing was observed for both silver-containing samples. The composites containing silver nanoparticles are characterized by different locations of SPR maxima depending on the substrate type. The SPRs of Ag:SG and Ag:SLSG were located at 415 and 440 nm, respectively. The doubled frequency of laser radiation ($\lambda = 1064$ nm) is smaller than the SPR frequencies of Ag nanoparticles in both matrixes, which corresponds to a positive sign of the refractive nonlinearity.

The output characteristics of second-harmonic radiation were as follows: $t = 55$ ps, $E = 0.26$ mJ, and $\lambda = 532$ nm. Figure 3a shows the normalized transmittance dependencies of silver-doped SLSG and silver-doped SG samples measured using the open-aperture z-scan scheme at $I_0 = 2.5 \times 10^9$ W cm^{-2}. The transmission of samples was increased due to saturated absorption as they were approaching close to the focal plane.

After the fitting of theoretical curves with experimental data the nonlinear absorption coefficients of Ag:SLSG and Ag:SG were calculated to be -6.7×10^{-5} and -3.6×10^{-5} cm W^{-1}, respectively. The relation between the nonlinear absorption coefficient and saturated intensity can be written as $\beta = -\alpha_0/I_s$. The I_s was evaluated for these two samples

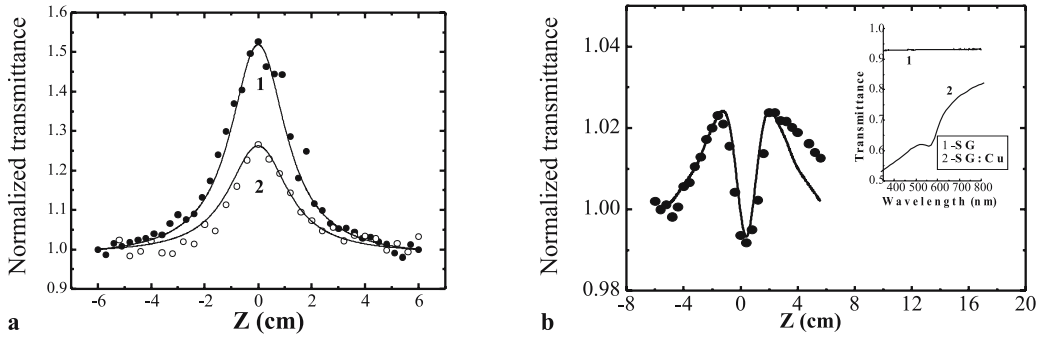

FIGURE 3 (**a**) Normalized transmittance dependencies of (1) Ag:SLSG, and (2) Ag:SG in the case of open-aperture z-scan scheme at the laser radiation intensity of $I_0 = 2.5 \times 10^9$ W cm^{-2}. *Solid lines* show the theoretical fits. (**b**) Normalized transmittance as a function of Cu:SG position in the case of the open-aperture z-scan scheme ($I_0 = 5.4 \times 10^9$ W cm^{-2}). *Solid line* is the theoretical fit. *Inset*: Transmission spectra of SG (1) before and (2) after implantation of copper ions

to be $1.1 \times 10^9\,\mathrm{W\,cm^{-2}}$ (Ag:SLSG) and $1.4 \times 10^9\,\mathrm{W\,cm^{-2}}$ (Ag:SG).

The open-aperture $T(z)$ dependence of Cu:SG sample (Fig. 3b) can be explained in terms of the concurrency of positive and negative absorption nonlinearities, which arose from the excited state absorption. The best theoretical fit in that case was obtained with $\beta = 6 \times 10^{-6}\,\mathrm{cm\,W^{-1}}$ and $I_\mathrm{s} = 4.3 \times 10^8\,\mathrm{W\,cm^{-2}}$.

The normalized transmittance dependencies of Ag:SLSG and Ag:SG samples obtained using a closed-aperture scheme at $I_0 = 2.5 \times 10^9\,\mathrm{W\,cm^{-2}}$ showed a negative value of the nonlinear refractive index at $\lambda = 532\,\mathrm{nm}$. From the fits of the theoretical curves and experimental data the values of γ and $\mathrm{Re}\chi^{(3)}$ were calculated to be $-4.1 \times 10^{-10}\,\mathrm{cm^2\,W^{-1}}$ and -2.4×10^{-8} esu for Ag:SLSG, and $-6.2 \times 10^{-10}\,\mathrm{cm^2\,W^{-1}}$ and -3.5×10^{-8} esu for Ag:SG.

Nonlinear optical studies of metal nanoparticles were generally carried out in the visible and near IR ranges. At the same time such structures can possess interesting nonlinear optical properties in the UV range. The parameters of the third-harmonic radiation of the Nd:YAG laser, which we used in our studies of silver- and copper-doped glasses in the UV range, were as follows: $t = 55\,\mathrm{ps}$, $E = 0.1\,\mathrm{mJ}$, $\lambda = 354.7\,\mathrm{nm}$. The normalized transmittance dependence in the closed-aperture scheme showed a negative sign of the nonlinear refraction for the Ag:SG sample. An observed asymmetry of this dependence, where peaks exceed valleys, characterizes a saturated absorption in the sample. From the fit of the theoretical calculations and experimental data the nonlinear optical parameters were found to be $\gamma = -7.6 \times 10^{-10}\,\mathrm{cm^2\,W^{-1}}$ and $\beta = -1.4 \times 10^{-5}\,\mathrm{cm\,W^{-1}}$ for Ag:SG. A corresponding value of $\mathrm{Im}\chi^{(3)}$ was calculated to be -2.7×10^{-9} esu. For comparison, an analogous parameter for Ag nanocrystal-glass composite, though at the smaller volume part, was previously reported to be -0.8×10^{-10} esu in the same spectral region [17]. Taking into account a definition of the third-order nonlinear optical susceptibility of nanoparticles [18], the latter value for silver nanoparticles was comparable in our and previous work [17]. The same measurements for Cu:SG allowed determining $\gamma = -1.7 \times 10^{-10}\,\mathrm{cm^2\,W^{-1}}$ and $\beta = -6.7 \times 10^{-6}\,\mathrm{cm\,W^{-1}}$.

4.4 *Cobalt-doped polyvinylpyrrolidone*

Here we present the results of the study of cobalt nanoparticles-doped polyvinylpyrrolidone (PVP). PVP has the advantage of accepting high concentrations of various guest molecules and atoms without the loss of its good optical properties (in particular a negligible scattering). Aqueous solutions of the Co-doped PVP at different concentrations of cobalt (2, 5.3, 6.2 and 13.5 wt. %) were used. We did not carry out the direct measurements of the sizes of Co nanoparticles. However, the absorption measurements of Co-doped PVP showed a characteristic absorption peak near the surface plasmon resonance of cobalt nanoparticles (525 nm).

The investigations of the nonlinear optical characteristics of the Co-doped PVP solutions were carried out at the wavelengths of 1064 and 532 nm ($t = 35\,\mathrm{ps}$). The nonlinear refractive indices of the 13.5% cobalt-doped PVP solution were measured to be -3.6×10^{-15} and $-2.7 \times 10^{-14}\,\mathrm{cm^2\,W^{-1}}$

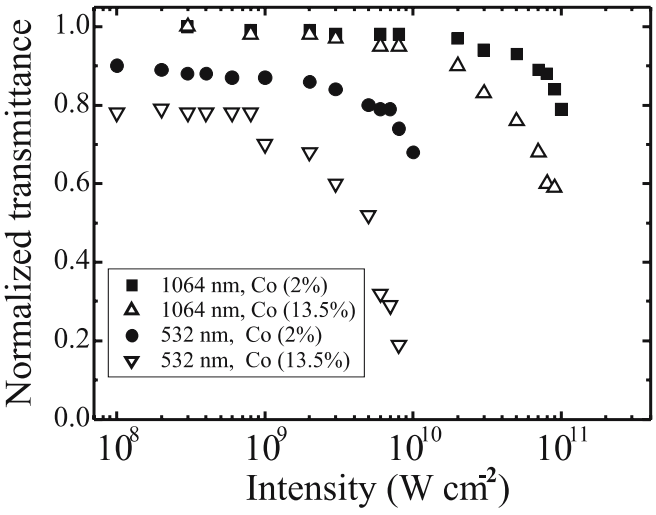

FIGURE 4 Normalized transmittances of Co nanoparticle-doped PVP as a functions of the laser radiation intensity at the wavelengths of 532 and 1064 nm

at 1064 and 532 nm, respectively. The nonlinear absorption studies showed that this process was observed only at $\lambda = 532\,\mathrm{nm}$. A decrease of transmittance at the wavelength of 532 nm was due to the reverse saturated absorption, which was manifested in a number of organometallic and polymer structures in the visible range [19]. The nonlinear absorption of 13.5% cobalt-PVP solution was measured to be $3.2 \times 10^{-9}\,\mathrm{cm\,W^{-1}}$.

Figure 4 shows the dependencies of the normalized transmittance of cobalt-doped PVP solutions at different laser intensities in the case of a closed-aperture scheme. In the case of $\lambda = 1064\,\mathrm{nm}$ the solution-containing cell was kept in the region of lowest transmittance and the optical limiting was attributed to the self-defocusing. Another picture was observed at the wavelength of 532 nm. In this case the optical limiting was attributed to both the self-defocusing and nonlinear absorption. The nonlinear absorption can be explained by the influence of both two-photon absorption and reverse saturated absorption (at high intensities).

5 Semiconductor nanoparticles (GaAs, CdS, As_2S_3)

Laser ablation is an effective technique for the preparation of semiconductor nanoparticle suspensions. The local field enhancement of nanoparticles in colloidal suspensions and the considerable nonlinear optical susceptibilities of chalcogenide structures, can lead to the interesting features of such semiconductor nanoparticles prepared by laser ablation. This technique was used for the preparation and investigation of aqueous colloidal suspensions of As_2S_3 and CdS nanoparticles.

A Q-switched Nd:YAG laser ($\lambda = 1064\,\mathrm{nm}$, $t = 20\,\mathrm{ns}$, $E = 15\,\mathrm{mJ}$) operating at a 10 Hz pulse repetition rate was used for the laser ablation of As_2S_3 and CdS semiconductors. The samples (bulk As_2S_3 or CdS) were placed in a quartz cell containing distilled water and irradiated for 15–25 min. This technique allowed synthesis of semiconductor nanoparticles with sizes of 2–8 nm. The volume ratio of nanoparticles in the suspensions was estimated to be 4×10^{-5}. The observed

UV absorption edge of the synthesized CdS nanoparticles ($\lambda = 320$ nm, $E_g = 3.86$ eV) was blue-shifted in comparison to that of bulk CdS ($\lambda = 490$ nm, $E_g = 2.53$ eV), thus confirming the formation of nanoparticles in suspensions. The same properties were observed in the case of As_2S_3 nanoparticle suspensions. The TEM analysis also confirmed the presence of nanoparticles.

The value of γ for CdS suspension at $\lambda = 532$ nm was calculated from the closed-aperture z-scans to be 4×10^{-15} cm^2 W^{-1}. The small values of nonlinear optical parameters of these suspensions were caused by the low concentration of nanoparticles. However, taking into account the volume ratio of semiconductor nanoparticles, we estimated that their nonlinearities exceeded those of bulk materials.

The analysis of the sign of the nonlinear refraction of semiconductor nanoparticle suspensions was carried out using Kramers–Kronig transformations. Such nanostructures, for instance CdS, can exhibit the other sign of γ compared to that for bulk CdS at $\lambda = 532$ nm. The intrinsic measure of the size at which the variations of nonlinear optical processes begin to become important is given by the diameter of the 1S exciton in bulk crystalline material [20]. For CdS, this diameter is 6 nm. The calculations of the shift of the band gap for different sizes of CdS nanoparticles were reported in [20]. We assumed that the influence of small nanoparticles can change the sign of the nonlinear process (from self-defocusing to self-focusing). In our case the $\hbar\omega/E_g$ becomes equal to 0.65, which corresponds to the positive sign of γ. These assumptions were confirmed by our observations, which have shown the change of sign of the nonlinear optical process in the case of small nanoparticles.

An analogous consideration was carried out for As_2S_3 suspension. Its energy band gap shifted from 2.37 eV (bulk As_2S_3) to 3.19 eV (semiconductor suspension). The absorption cut-off in that case was not as evident as in the case of the CdS suspension, indicating a broader size distribution of As_2S_3 nanoparticles.

In the next set of studies we analyzed the GaAs nanoparticles ablated in various liquids. Laser ablation of GaAs was carried out using the second-harmonic radiation of the Nd:YAG laser. The volume ratio of GaAs in the liquid suspensions was estimated to be 2×10^{-4}. The TEM measurements conducted just after laser ablation showed the appearance of long-sized nanoparticles. The nanoparticles distribution was considerably narrowed after the sedimentation of long-sized nanoparticles (as in the case of silver ablation) with the small nanoparticles (ranging from 5 to 15 nm) dominating in the GaAs suspension.

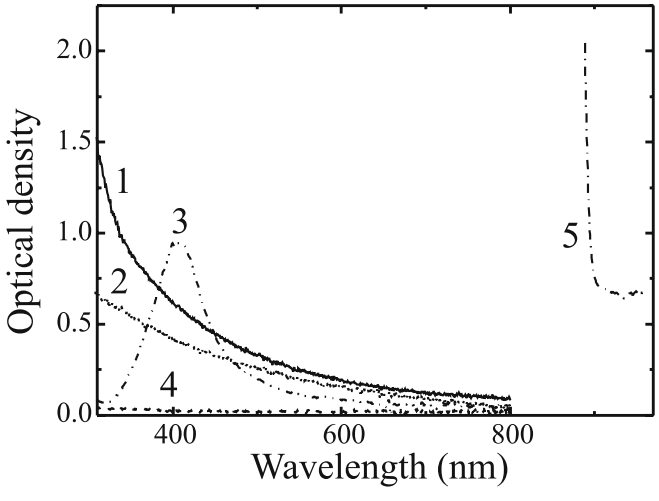

FIGURE 5 Absorption spectra of 10 mm thick GaAs:EG suspension (1) one and (2) three weeks after ablation, (3) silver:EG suspension, (4) pure ethylene glycol, and (5) 500 μm thick bulk GaAs wafer

The absorption spectra of suspensions were similar to those of quantum-confined GaAs nanocrystals embedded in glasses [21], exhibiting a broad absorption throughout the visible and UV ranges. Figure 5, curve 1, shows the absorption spectrum of GaAs nanoparticles suspended in ethylene glycol (GaAs:EG). The absorption curve was considerably blue-shifted compared to that of the bulk GaAs (curve 5). The effect of liquid degradation inside the focal volume was negligible in the case of water, ethanol, and ethylene glycol since our observations of silver ablation in analogous conditions have shown an absorption spectrum, which can be attributed to the SPR of silver (curve 3). However, in the case of silicon oil we observed its degradation during the ablation of both GaAs and Ag. The variations of the absorption spectra of GaAs nanoparticles in water, ethylene glycol, and ethanol induced by the sedimentation of long nanoparticles were observed for a period of one month (curves 1 and 2). In the case of the GaAs ablated in silicon oil, the nanoparticle size distribution and absorption spectra remained constant for a long time due to the high viscosity of the host material. In that case we observed an inhomogeneous distribution of GaAs particles ranging from big blocks (0.2–10 μm) to nanoparticle-sized structures.

The beam shape variations in the far field in the case of GaAs:EG suspension obtained using the radiation of a Ti:sapphire oscillator ($\lambda = 795$ nm, $W = 300$ mW, $t = 100$ fs, 80 MHz pulse repetition rate) allowed analysis of the influence of thermally induced nonlinearities. A strong thermally induced self-defocusing was clearly seen in the CCD images. At $z = z_1$, the self-defocusing concentrated radiation in the far field. At $z = z_2$, the self-defocusing led to the appearance of a ring-shaped beam. The z_1 and z_2 positions correspond to the peak and valley of normalized transmittance in the case of the closed-aperture z-scan. The thermally induced nonlinear refractive index of GaAs:EG suspension was measured to be $\gamma = -4 \times 10^{-13}$ cm^2 W^{-1}.

The application of short laser pulses (in picosecond and femtosecond ranges) at low pulse repetition rates allows the exclusion of the influence of slow thermally induced nonlinear optical processes and analysis of the self-interaction mechanisms caused by the electronic response of GaAs nanoparticles. Our studies using 795 and 397 nm radiation of a femtosecond laser were performed at intensities up to $I_0 = 1 \times 10^{11}$ W cm^{-2}, however, we did not register the influence of GaAs nanoparticles on the nonlinear refractive properties of GaAs:liquid suspensions. The only nonlinear optical process in GaAs nanoparticle-containing suspensions was a nonlinear absorption at 795 nm due to two-photon processes in these compounds. After fitting the theoretical curve with experimental data, the nonlinear absorption co-

efficient of GaAs:water suspension was calculated to be 0.7×10^{-9} cm W^{-1}.

6 Discussion and conclusions

The real values of the nonlinear susceptibilities of nanoparticles are considerably higher that those of the solutions. A simple and well-established method for the estimation of the nonlinear susceptibilities of nanoparticles is to divide the nonlinear susceptibility of compound by the volume part of nanoparticles. The $\chi^{(3)}$ values of composites are enhanced by the fourth power of the local field factor as

$$\chi^{(3)} = p|f_l|^2 f_l^2 \chi_n^{(3)}, \quad (8)$$

where $\chi_n^{(3)}$ is the third-order nonlinear susceptibility of nanoparticles, f_l is the local field factor, and p is the volume fraction of nanoparticles [22]. The same procedure can be applied to the definition of the nonlinear refractive indices and nonlinear absorption coefficients of nanoparticles.

The volume part of Ag nanoparticles in the liquids was measured to be 4×10^{-5}, from where the nonlinear susceptibility of the Ag nanoparticles were defined to be 5×10^{-8} esu. The same can be said in the case of GaAs suspensions. From the data of the volume part of GaAs nanoparticles in the suspensions (2×10^{-4}) and the nonlinear absorption coefficient of GaAs:water suspension (7×10^{-10} cm W^{-1}) one can calculate the nonlinear absorption coefficient induced by GaAs nanoparticles (3.5×10^{-6} cm W^{-1}).

In the case of the metal colloidal suspensions (Ag, Au, Cu, Pt) prepared by chemical methods, the estimated volume part of metal nanoparticles was in the range of 10^{-3}. The corresponding nonlinear absorption coefficients and nonlinear refractive indices of metal nanoparticles were estimated to be 9.4×10^{-9} cm W^{-1} (Au nanoparticles) and -9×10^{-10} cm W^{-2} (Ag nanoparticles).

The volume part of the Ag and Cu nanoparticles doped in glass matrices using the beam implantation was estimated to be in the range of 5×10^{-2} in the thin under-surface layer (60 nm). The corresponding value of γ of these nanoparticles was estimated to be in the range of 2×10^{-9} cm^2 W^{-1}, while the nonlinear susceptibility of nanoparticles was calculated to be 0.5×10^{-6} esu.

In the case of 13.5% cobalt nanoparticle-doped PVP solution, the nonlinear refractive indices of Co nanoparticles were measured to be -3×10^{-14} and -2×10^{-13} cm^2 W^{-1} (at 1064 and 532 nm, respectively), while the nonlinear absorption coefficient of Co nanoparticles at 532 nm was calculated to be 2×10^{-8} cm W^{-1}.

The values of γ of the semiconductor nanoparticles (CdS, As_2S_3) dissolved in water were estimated to be in the range of 10^{-10} cm^2 W^{-1}, taking into account the volume part of these species in aqueous solution (4×10^{-5}).

All these measurements and estimations of the nonlinear optical parameters of nanoparticles have shown that, in some cases, they possess high nonlinear refraction, absorption and susceptibility (up to 2×10^{-9} cm^2 W^{-1}, 3×10^{-6} cm W^{-1}, and 5×10^{-7} esu, respectively). These values are almost three orders of magnitude higher compared to those measured from various bulk media. This study confirmed the involvement of quantum size effects in the growth of the nonlinear optical response of small-sized particles.

In conclusion, we have presented studies of the nonlinear optical properties of various nanoparticle-containing media using the laser radiation generated in different spectral and temporal ranges. The basic mechanisms involved in each class of nanoparticle-containing materials are quite different. However, among the mechanisms involved in the case of different samples, the Kerr-induced self-interaction, excited state saturation, reverse saturates absorption, and multiphoton absorption play crucial roles in the variation of refractive indices and absorption of these media. The observed positive sign of the nonlinear refraction of As_2S_3 and CdS nanoparticle suspensions was discussed, and an explanation based on size-related effective band gap variations was offered. The simultaneous appearance of saturated and reverse saturated absorption was observed in the case of some metal nanoparticles doped in silica glasses and stabilizers, as well as colloidal suspensions of various metals. Our studies of nanoparticle-containing media confirmed a considerable nonlinear optical response of these structures, especially in the vicinity of their SPRs.

ACKNOWLEDGEMENTS The authors are indebted to T. Usmanov, I.A. Kulagin, R.I. Tugushev, and S.R. Kamalov from NPO Akadempribor, Tashkent, Uzbekistan and H. Kuroda, M. Baba, and M. Suzuki from the Institute for Solid State Physics, University of Tokyo, Japan for the collaboration. We also thank A.L. Stepanov for providing the metal-doped glass samples for these studies.

REFERENCES

1 U. Kreibig, M. Vollmer, *Optical Properties of Metal Clusters* (Springer, Berlin, 1995)
2 L.W. Tutt, A. Kost, Nature **356**, 225 (1992)
3 W. Ji, H.J. Du, S.H. Tang, S. Shi, J. Opt. Soc. Am. B **12**, 876 (1995)
4 J. Staromlynska, T.J. McKay, P. Wilson, J. Appl. Phys. **88**, 1726 (2000)
5 X. Lui, S. Guo, H. Wang, L. Hou, Opt. Commun. **197**, 431 (2001)
6 R.A. Ganeev, M. Baba, A.I. Ryasnyansky, M. Suzuki, M. Turu, H. Kuroda, Appl. Phys. B **78**, 433 (2004)
7 H. Toda, C.M. Verber, Opt. Lett. **17**, 1379 (1992)
8 R.A. Ganeev, M. Baba, M. Morita, A.I. Ryasnyansky, M. Suzuki, H. Kuroda, J. Opt. A **6**, 1076 (2004)
9 J.F. Reintjes, *Nonlinear Optical Parametric Processes in Liquids and Gases* (Academic Press, Orlando, 1984)
10 I.A. Kulagin, T. Usmanov, Quantum Electron. **28**, 1092 (1998)
11 A. Ricard, P. Raussignol, C. Flytzanis, Opt. Lett. **10**, 511 (1985)
12 J. Olivares, J. Requejo-Isidro, R. Del Coso, R. De Nalda, J. Solis, C.N. Afonso, A.L. Stepanov, D. Hole, P.D. Townsend, A. Naudon, J. Appl. Phys. **90**, 1064 (2001)
13 M. Baba, M. Ichihara, R.A. Ganeev, M. Suzuki, H. Kuroda, M. Morita, D. Rau, T. Ishii, M. Iwamura, Appl. Phys. Lett. **84**, 2394 (2004)
14 Y.-P. Sun, J.E. Riggs, H.W. Rollins, R. Guduru, J. Phys. Chem. B **103**, 77 (1999)
15 A.L. Stepanov, D.E. Hole, Recent Res. Dev. Appl. Phys. **5**, 1 (2002)
16 A.L. Stepanov, D.E. Hole, P.D. Townsend, J. Non-Cryst. Solids **260**, 65 (1999)
17 Y. Hamanaka, A. Nakamura, N. Hayashi, S. Omi, J. Opt. Soc. Am. B **20**, 1227 (2003)
18 F. Hache, D. Ricard, C. Flytzanis, J. Opt. Soc. Am. B **3**, 1647 (1986)
19 J.W. Perry, K. Mansour, S.R. Marder, K.J. Perry, D. Alverez, L. Choong, Opt. Lett. **19**, 625 (1994)
20 R. Rossetti, J.L. Ellison, J.M. Gibson, L.E. Brus, J. Chem. Phys. **80**, 4464 (1984)
21 L. Justus, R.J. Tonucci, A.D. Berry, Appl. Phys. Lett. **61**, 3151 (1992)
22 K. Uchida, S. Kaneko, S. Omi, C. Hata, H. Tanji, Y. Asahara, A.J. Ikushima, T. Tokizaki, A. Nakamura, J. Opt. Soc. Am. B **11**, 1236 (1994)